Chapter 15
Locally Specified Polygonal Markov Fields for Image Segmentation

Michal Matuszak and Tomasz Schreiber

Abstract We introduce a class of polygonal Markov fields driven by local activity functions. Whereas the local rather than global nature of the field specification ensures substantial additional flexibility for statistical applications in comparison to classical polygonal fields, we show that a number of simulation algorithms and graphical constructions, as developed in our previous joint work with M.N.M. van Lieshout and R. Kluszczynski, carry over to this more general framework. Moreover, we provide explicit formulae for the partition function of the model, which directly implies the availability of closed form expressions for the corresponding likelihood functions. Within the framework of this theory we develop an image segmentation algorithm based on Markovian optimization dynamics combining the simulated annealing ideas with those of Chen-style stochastic optimization, in which successive segmentation updates are carried out simultaneously with adaptive optimization of the local activity functions.

15.1 Introduction

The polygonal Markov fields, originally introduced by Arak and Surgailis [10–12] and then studied by a number of authors [13, 319, 377–379, 395], arise as continuum ensembles of non-intersecting polygonal contours in the plane. One of the sources of theoretical interest in these processes lies in that they share a number of salient features with the two-dimensional Ising model, including the geometry of phase transitions and phase separation phenomenon [319, 377, 378] as well as the availability of explicit formulae for important numerical characteristics [11, 12, 379] yielding in particular closed form expressions for the likelihood functions. The idea that the polygonal Markov fields can carry out image processing tasks traditionally reserved for lattice-indexed Markov fields (see [448] for a comprehensive survey, cf.

M. Matuszak (✉) · T. Schreiber
Faculty of Mathematics & Computer Science, Nicolaus Copernicus University,
ul. Chopina 12/18, 87-100 Toruń, Poland
e-mail: gruby@mat.uni.torun.pl

T. Schreiber
e-mail: tomeks@mat.uni.torun.pl

L. Florack et al. (eds.), *Mathematical Methods for Signal and Image Analysis and Representation*, Computational Imaging and Vision 41,
DOI 10.1007/978-1-4471-2353-8_15, © Springer-Verlag London Limited 2012

also Chap. 14 and the references therein for new developments) has emerged quite early and originates from Clifford, Middleton and Nicholls [79] who formulated it in a Bayesian setting. The obvious crucial advantage of polygonal fields in this context is their continuum nature which makes them completely free of lattice artifacts in image processing applications. The significant problem which slowed down the progress of this early work was the lack of efficient samplers and simulation algorithms for polygonal fields. These were introduced a decade later in a series of our joint papers with M.N.M. van Lieshout and R. Kluszczynski [256, 257, 377, 380, 424] where a polygonal field optimization approach for image segmentation was advocated. Although these methods were quite succesful in global shape recognition, the problem we faced in that work was related to the lack of local parametrization tools designed to deal with intermediate scale image characteristics—even though the applied simulated annealing algorithm would eventually converge to the target polygonal segmentation, we were looking for a more efficient explicit mechanism to drive the local search. Introducing such mechanisms and applying them to image segmentation is the principal purpose of the present paper. We construct a class of polygonal Markov fields with local activity functions (Sect. 15.2) and discuss their properties and graphical representations (Sect. 15.3). Next, in Sects. 15.4 and 15.5 we develop a Markovian optimization dynamics for image segmentation, under which both the polygonal configuration and the underlying local activity function are subject to optimization—whereas the polygonal configuration evolves according to a simulated annealing scheme in the spirit of [256, 257], the local activity function is initially chosen to reflect the image gradient information, whereupon it undergoes adaptive updates in the spirit of the celebrated Chen algorithm, see [73] and 10.2.4.c. in [333], with the activity profile reinforced along polygonal paths contributing to the improvement of the overall segmentation quality and faded along paths which deteriorate the segmentation quality. The sample results of our software are presented in the final Sect. 15.6.

15.2 Locally Specified Polygonal Markov Fields

Fix an open bounded convex set D in the plane $\mathbb{R}^2$, referred to as the field domain in the sequel, and define the family Γ_D of admissible polygonal configurations in D, by taking all the finite planar graphs γ in $D \cup \partial D$, with straight-line segments as edges, such that

- The edges of γ do not intersect,
- All the interior vertices of γ (lying in D) are of degree 2,
- All the boundary vertices of γ (lying in ∂D) are of degree 1,
- No two edges of γ are colinear.

In other words, γ consists of a finite number of disjoint polygons, possibly nested and chopped off by the boundary. We shall write $\Gamma_D[k] \subset \Gamma_D$ for the set of all admissible polygonal configurations in D with precisely k edges.

For a Borel subset of $A \subseteq \mathbb{R}^2$ by $[\![A]\!]$ we shall denote the family of all straight lines hitting A so that in particular $[\![\mathbb{R}^2]\!]$ stands for the collection of all straight lines in $\mathbb{R}^2$. Further, we let μ be the standard isometry-invariant Haar-Lebesgue measure on the space $[\![\mathbb{R}^2]\!]$ of straight lines in $\mathbb{R}^2$. Recall that one possible construction of μ goes by identifying a straight line l with the pair $(\phi, \rho) \in [0, \pi) \times \mathbb{R}$, where $(\rho \sin(\phi), \rho \cos(\phi))$ is the vector orthogonal to l, and joining it to the origin, and then by endowing the parameter space $[0, \pi) \times \mathbb{R}$ with the usual Lebesgue measure. Note that the above parametrisation of $[\![\mathbb{R}^2]\!]$ with $[0, \pi) \times \mathbb{R}$ endows $[\![\mathbb{R}^2]\!]$ with a natural metric, topology and Borel σ-field which will be used in this paper.

On $[\![D]\!] \times D$ we consider a non-negative bounded *local activity function* $\mathscr{M}(\cdot\,;\cdot)$ which will determine the local activity structure of the polygonal field. Define the formal Hamiltonian $L^{\mathscr{M}} : \Gamma_D \to \mathbb{R}_+$ given by

$$L^{\mathscr{M}}(\gamma) := \sum_{e \in \mathrm{Edges}(\gamma)} \int_{l \in [\![e]\!]} \mathscr{M}(l; l \cap e)\mu(dl), \quad \gamma \in \Gamma_D. \tag{15.1}$$

We note that the energy function $L^{\mathscr{M}}$ should be regarded as an anisotropic environment-specific version of the length functional. Indeed, for a line l hitting a graph edge $e \in \mathrm{Edges}(\gamma)$ at their intersection point $x = l \cap e$, the local activity $\mathscr{M}(l; l \cap e)$ shall be interpreted as the likelihood of a new edge being created along l intersecting and hence fracturing at x the edge e in γ. Under this interpretation we see that, roughly speaking, the value of $\int_{l \in [\![e]\!]} \mathscr{M}(l; l \cap e)\mu(dl)$ determines how likely the edge e is to be fractured by another edge present in the environment. In other words, $L^{\mathscr{M}}(\gamma)$ determines *how difficult it is to maintain* the whole graph $\gamma \in \Gamma_D$ without fractures in the environment whose local activity profile is characterised by $\mathscr{M}(\cdot\,;\cdot)$—note that due to the anisotropy of the environment there may be graphs of a higher (lower) total edge length than γ and yet of lower (higher) energy and thus easier (more difficult) to maintain and to keep unfractured due to the lack (presence) of high local activity lines likely to fracture their edges. In the particular case where $\mathscr{M}$ is constant, $L^{\mathscr{M}}$ is readily verified to be a multiple of the usual length functional, see e.g. p. 554 in [11].

We assume that a measurable *anchor mapping* $\mathbb{A} : [\![D]\!] \to D$ is given on the set of lines crossing D, assigning to each of them its *anchor point*, also interpreted as the *initial point* of the line. This allows us to define for each bounded linear segment/graph edge e in D its initial point $\iota[e]$ which is the point of e closest to the anchor $\mathbb{A}(l[e])$, where $l[e]$ is the straight line extending e. In particular, if $\mathbb{A}(l[e]) \in e$ then $\iota[e] = \mathbb{A}(l[e])$, otherwise $\iota[e]$ is the endpoint of e closest to $\mathbb{A}(l[e])$.

The polygonal Markov field $\mathscr{A}_D^{\mathscr{M}}$ with local activity function $\mathscr{M}$ in D is defined by

$$\begin{aligned} &\mathbb{P}(\mathscr{A}_D^{\mathscr{M}} \in d\gamma) \\ &\quad \propto \exp(-L^{\mathscr{M}}(\gamma)) \prod_{e \in \mathrm{Edges}(\gamma)} [\mathscr{M}(l[e]; \iota[e])\mu(dl[e])], \quad \gamma \in \Gamma_D. \end{aligned} \tag{15.2}$$

In other words, the probability of having $\mathscr{A}_D^{\mathscr{M}} \in d\gamma$ is proportional to the Boltzmann factor $\exp(-L^{\mathscr{M}}(\gamma))$ times the product of local edge activities $\mathscr{M}(l[e];$

$\iota[e])\mu(dl[e])$, $e \in \mathrm{Edges}(\gamma)$. Observe that this construction should be regarded as a specific version of the general polygonal model given by Arak and Surgailis [11, 2.11] and an extension of the non-homogeneous polygonal fields considered in Schreiber [379] at their consistent regime (inverse temperature parameter fixed to 1). It should be also noted at this point that if the typical edge length for $\mathscr{A}_D^{\mathscr{M}}$ is much smaller than the characteristic scale for oscillations of $\mathscr{M}$, which is often the case in our applications below, then $\mathscr{M}(l[e];\cdot)$ is usually approximately constant along the corresponding edge e and the formal dependency of the factor $\mathscr{M}(l[e];\iota[e])\mu(dl[e])$ on the choice of initial segment for e becomes negligible in large systems. The finiteness of the partition function

$$\mathscr{Z}_D^{\mathscr{M}} := \sum_{k=0}^{\infty} \frac{1}{k!} \int_{\Gamma_D[k]} \exp(-L^{\mathscr{M}}(\gamma)) \prod_{e\in\mathrm{Edges}(\gamma)} [\mathscr{M}(l[e];\iota[e])\mu(dl[e])] \tag{15.3}$$

is not difficult to verify, see [379], and in fact it will be explicitly calculated in the sequel.

The so-defined locally specified polygonal fields enjoy a number of striking features inherited from the previously developed polygonal models, see [11, 379]. One of these is the two-dimensional germ-Markov property stating that the conditional behaviour of the field $\mathscr{A}_D^{\mathscr{M}}$ inside a smooth closed curve θ depends on the outside field configuration only through the trace it leaves on θ, consisting of intersection points and the respective line directions, see [11] for details. This is where the term *polygonal Markov field* comes from. Further properties of the locally defined polygonal fields are going to be discussed in the next section, where their algorithmic construction is provided.

15.3 Dynamic Representation for Locally Specified Polygonal Fields

The present section is meant to extend the so-called *generalised dynamic representation* for consistent polygonal fields as developed in Schreiber [379] to cover the more general class of locally specified polygonal fields defined in Sect. 15.2 above. The name *generalised representation* comes from the fact that it generalises the original construction of homogeneous polygonal fields introduced by Arak and Surgailis [11]. In the sequel we will often omit the qualifier *generalised* for the sake of terminological brevity. To describe the generalised representation, fix the convex field domain D and let $(D_t)_{t\in[0,1]}$ be a time-indexed increasing family of compact convex subsets of $\bar{D}$, eventually covering the entire $\bar{D}$ and interpreted as a *growing window* gradually revealing increasing portions of the polygonal field under construction in the course of the time flow. In other words, under this interpretation, the portion of a polygonal field in a bounded open convex domain D *uncovered* by time t is precisely its intersection with D_t. To put it in formal terms, consider $(D_t)_{t\in[0,1]}$ satisfying

(D1) $(D_t)_{t\in[0,1]}$ is a strictly increasing family of compact convex subsets of $\bar{D} = D \cup \partial D$.
(D2) D_0 is a single point x in $\bar{D} = D \cup \partial D$.
(D3) D_1 coincides with $\bar{D}$.
(D4) D_t is continuous in the usual Hausdorff metric on compacts.

Clearly, under these conditions, for μ-almost each $l \in [\![D]\!]$ the intersection $l \cap D_{\tau_l}$ consists of precisely one point $\mathbb{A}(l)$, where $\tau_l = \inf\{t \in [0,1],\ D_t \cap l \neq \emptyset\}$. The point $\mathbb{A}(l)$ is chosen to be the *anchor point* for l, which induces the *anchor* mapping $\mathbb{A} : [\![D]\!] \to D$ as required for our construction in Sect. 15.2. Note that this choice of the anchor mapping implies that at each point of a line l the direction away from its anchor point $\mathbb{A}(l)$ coincides with the outwards direction with respect to the *growing window* (D_t). Consider now the following dynamics in time $t \in [0,1]$, with all updates, given by the rules below, performed independently of each other, see Fig. 15.1.

(*GE:Initialise*) Begin with empty field at the time 0.
(*GE:Unfold*) Between critical moments listed below, during the time interval $[t, t+dt]$ the unfolding field edges in D_t reaching ∂D_t extend straight to $D_{t+dt} \setminus D_t$.
(*GE:BoundaryHit*) When a field edge hits the boundary ∂D, it stops growing in this direction (note that μ-almost everywhere the intersection of a line with ∂D consists of at most two points).
(*GE:Collision*) When two unfolding field edges intersect in $D_{t+dt} \setminus D_t$, they are not extended any further beyond the intersection point (stop growing in the direction marked by the intersection point).
(*GE:DirectionalUpdate*) A field edge extending along $l \in [\![D_t]\!]$ updates its direction during $[t, t+dt]$ and starts unfolding along $l' \in [\![l^{[t,t+dt]}]\!]$, extending away from the anchor point $\mathbb{A}(l')$, with probability $\mathscr{M}(l'; l \cap l')\mu(dl')$, where $l^{[t,t+dt]} := l \cap (D_{t+dt} \setminus D_t)$. Directional updates of this type are all performed independently.
(*GE:LineBirth*) Whenever the anchor point $\mathbb{A}(l)$ of a line l falls into $D_{t+dt} \setminus D_t$, the line l is born at the time t at its anchor point with probability $\mathscr{M}(l; \mathbb{A}(l))\mu(dl)$, whereupon it begins extending in both directions with the growth of D_t (recall that l is μ-almost always tangential to ∂D_t here).
(*GE:VertexBirth*) For each intersection point of lines l_1 and l_2 falling into $D_{t+dt} \setminus D_t$, the pair of field lines l_1 and l_2 is born at $l_1 \cap l_2$ with probability $\mathscr{M}(l_1; l_1 \cap l_2)\mathscr{M}(l_2; l_1 \cap l_2)\mu(dl_1)\mu(dl_2)$, whereupon both lines begin unfolding in the directions away from their respective anchor points $\mathbb{A}(l_1)$ and $\mathbb{A}(l_2)$.

Observe that the evolution rule (*GE:VertexBirth*) means that pairs of lines are born at birth sites distributed according to a Poisson point process in D with intensity measure given by the *intersection measure* $\langle\!\langle \mathscr{M} \rangle\!\rangle$ of $\mathscr{M}$:

$$\langle\!\langle \mathscr{M} \rangle\!\rangle(A) := \frac{1}{2} \int_{\{(l_1,l_2),\, l_1 \cap l_2 \subset A\}} \mathscr{M}(l_1; l_1 \cap l_2)\mathscr{M}(l_2; l_1 \cap l_2)\mu(dl_1)\mu(dl_2). \quad (15.4)$$

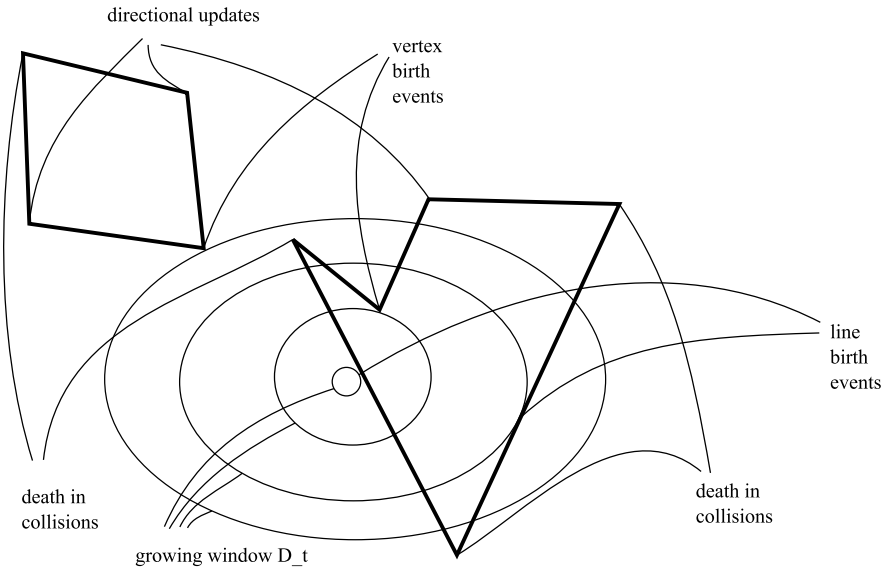

Fig. 15.1 Dynamic representation

Likewise, the evolution rule (*GE:LineBirth*) implies that individual lines are born at their anchor points according to a Poisson point process in $[\![D]\!]$ with intensity measure given by the *anchor measure* $\langle \mathscr{M} \rangle$ of $\mathscr{M}$:

$$\langle \mathscr{M} \rangle(B) := \int_{\{l,\, \mathbb{A}(l) \in B\}} \mathscr{M}(l, \mathbb{A}(l))\mu(dl). \tag{15.5}$$

The main theorem of this section is the following extension of Theorem 3 in [379].

Theorem 15.1 *The random contour ensemble resulting from the above construction* (*GE*) *coincides in law with* $\mathscr{A}_D^{\mathscr{M}}$. *Moreover, we have*

$$\log \mathscr{Z}_D^{\mathscr{M}} = \langle\langle \mathscr{M} \rangle\rangle(D) + \langle \mathscr{M} \rangle([\![D]\!]). \tag{15.6}$$

Proof We pick some $\gamma \in \Gamma_D$ and calculate the probability that the outcome of the above dynamic construction falls into $d\gamma$. To this end, we note that:

- Each edge $e \in \mathrm{Edges}(\gamma)$ containing the anchor point $\mathbb{A}(l[e])$ and hence resulting from a line birth event due to the rule (*GE:LineBirth*), contributes to the considered probability the factor $\mathscr{M}(l[e]; \mathbb{A}(l[e]))\mu(dl[e])$ (line birth probability for $l[e]$) times $\exp[-\int_{[\![e]\!]} \mathscr{M}(l; l \cap e)\mu(dl)]$ (no directional updates along e).
- Each of the two edges $e_1, e_2 \in \mathrm{Edges}(\gamma)$ stemming from a common interior birth vertex $l[e_1] \cap l[e_2] = \iota[e_1] = \iota[e_2]$ yields the factor $\mathscr{M}(l[e_i]; \iota[e_i])\mu(dl[e_i])$, $i = 1, 2$, (coming from the vertex birth probability due to the rule (*GE:VertexBirth*)) times $\exp[-\int_{[\![e_i]\!]} \mathscr{M}(l; l \cap e_i)\mu(dl)]$ (no directional updates along e_i).

- Each of the edges $e \in \mathrm{Edges}(\gamma)$ arising in (*GE:DirectionalUpdate*) yields the factor $\mathscr{M}(l[e]; \iota[e])$ (directional update probability) times $\exp[-\int_{[\![e]\!]} \mathscr{M}(l; l \cap e)\mu(dl)]$ (no directional updates along e).
- The absence of interior birth sites in $D \setminus \gamma$ yields the factor $\exp[-\langle\!\langle \mathscr{M} \rangle\!\rangle(D)]$.
- Finally, the absence of line birth events for all lines in $[\![D]\!]$ except for the finite collection $\{l[e],\ e \in \mathrm{Edges}(\gamma),\ \mathbb{A}(l[e]) \in e\}$ yields the additional factor $\exp[\langle -\mathscr{M} \rangle([\![D]\!])]$.

Putting these observations together we conclude that the probability element of γ resulting from the generalized construction above is

$$\frac{\exp(-L^{\mathscr{M}}(\gamma)) \prod_{e \in \mathrm{Edges}(\gamma)} [\mathscr{M}(l[e]; \iota[e])\mu(dl[e])]}{\exp[\langle\!\langle \mathscr{M} \rangle\!\rangle(D)] \exp[\langle \mathscr{M} \rangle([\![D]\!])]}$$

and thus, upon comparing with (15.2) and (15.3), the field obtained by this construction coincides in law with $\mathscr{A}_D^{\mathscr{M}}$ as required and (15.6) follows as well. This completes the proof of the theorem. □

15.4 Disagreement Loop Dynamics

In this section we discuss a random dynamics on the space Γ_D of admissible polygonal configurations which leaves the law of the field $\mathscr{A}_D^{\mathscr{M}}$ invariant and reversible. This dynamics will be used in the sequel as a mechanism for update proposal generation in stochastic optimization schemes for image segmentation. We build upon [377, 379] in our presentation of the dynamics based on an important concept of a *disagreement loop*.

To proceed we place ourselves within the context of the dynamic representation discussed in Sect. 15.3 above and suppose that we observe a particular realisation $\gamma \in \Gamma_D$ of the polygonal field $\mathscr{A}_D^{\mathscr{M}}$ and that we modify the configuration by adding an extra (*GE:VertexBirth*) vertex birth site at $x_0 \in D$ to the existing collection of vertex births for γ, while keeping unchanged the remaining evolution rules (*GE*) for all the edges, including the two newly added ones. Denote the resulting new (random) polygonal configuration by $\gamma \oplus x_0$. A simple yet crucial observation is that for $x_0 \in D$ the symmetric difference $\gamma \triangle [\gamma \oplus x_0]$ is almost surely a single loop (a closed polygonal curve), possibly self-intersecting and possibly chopped off by the boundary (becoming a path then). Indeed, this is seen as follows. Each point in $x \in D$ can be attributed its *time coordinate* which is just the time moment at which x is first hit by ∂D_t. Then the chronologically initial point of the loop $\gamma \triangle [\gamma \oplus x_0]$ is of course x_0. Each of the two *new* polygonal curves p_1, p_2 initiated by edges e_1, e_2 emitted from x_0 unfold independently, according to (*GE*), each giving rise to a *disagreement path*. The initial segments of such a disagreement path correspond to the growth of the curve, say p_1, before its annihilation in the first collision. If this is a collision with the boundary, the disagreement path gets chopped off and terminates there. If this is a collision with a segment of the original configuration γ corresponding to a certain *old* polygonal curve p_3 emitted from a prior vertex birth

site, the *new* curve p_1 dies but the disagreement path continues along the part of the trajectory of p_3 which is contained in γ but not in $\gamma \oplus x_0$. At some further moment p_3 dies itself in γ, touching the boundary or killing another polygonal curve p_4 in γ. In the second case, however, this collision only happens for γ and not for $\gamma \oplus x_0$ so the polygonal curve p_4 survives (for some time) in $\gamma \oplus x_0$ yielding a further connected portion of the disagreement path initiated by p_1, which is contained in $\gamma \oplus x_0$ but not in γ etc. A recursive continuation of this construction shows that the disagreement path initiated by p_1 at x_0 consists alternately of connected polygonal sub-paths contained in $[\gamma \oplus x_0] \setminus \gamma$ (call these *creation phase* sub-paths) and in $\gamma \setminus [\gamma \oplus x_0]$ (call these *annihilation phase* sub-paths). Note that this disagreement path is self-avoiding and, in fact, it can be represented as the graph of some piecewise linear function $t \mapsto x(t) \in \partial D_t$. Clearly, the same applies for the disagreement path initiated by p_2 at x_0. An important observation is that whenever two *creation phase* or two *annihilation phase* sub-paths of the two disagreement paths hit each other, both disagreement paths die at this point and the disagreement loop closes (as opposed to intersections of segments of different phases which do not have this effect). Obviously, if the disagreement loop does not close in the above way, it gets eventually chopped off by the boundary. We shall write $\Delta^{\oplus}[x_0; \gamma] = \gamma \triangle [\gamma \oplus x_0]$ to denote the (random) disagreement loop constructed above. A similar argument shows that an extra (*GE:LineBirth*) line birth event added for $l \in [\![D]\!]$ at its anchor point $\mathbb{A}(l)$, while keeping the remaining evolution rules unchanged, also gives rise to a disagreement loop $\Delta^{\oplus}[l; \gamma]$ which coincides with the symmetric difference $\gamma \triangle [\gamma \oplus l]$, where $\gamma \oplus l$ is the polygonal configuration resulting from γ upon adding the line birth site at $\mathbb{A}(l)$.

Likewise, a disagreement loop arises if we *remove* one vertex birth site $x_0 \in D$ from the collection of vertex birth sites of an admissible polygonal configuration $\gamma \in \Gamma_D$, while keeping the remaining evolution rules. We write $\gamma \ominus x_0$ for the configuration obtained from γ by removing x_0 from the list of vertex birth sites, while the resulting random disagreement loop is denoted by $\Delta^{\ominus}[x_0; \gamma]$ so that $\Delta^{\ominus}[x_0; \gamma] = \gamma \triangle [\gamma \ominus x_0]$. In full analogy, we define $\gamma \ominus l$ and $\Delta^{\ominus}[l; \gamma]$ where $l = l[e]$ is the field line extending an edge $e \in \mathrm{Edges}(\gamma)$ with $\mathbb{A}(l) \in e$ and $\gamma \ominus l$ is the configuration obtained from γ upon killing the line l at its anchor $\mathbb{A}(l)$ whereas $\Delta^{\ominus}[x_0; \gamma]$ is the resulting disagreement loop. We refer the reader to Sect. 2.1 in [377] for further discussion.

With the above terminology we are in a position to describe a random dynamics on the configuration space Γ_D, which leaves invariant the law of the polygonal process $\mathscr{A}_D^{\mathscr{M}}$. Particular care is needed, however, to distinguish between the notion of time considered in the dynamic representation of the field as well as throughout the construction of the disagreement loops above, and the notion of time to be introduced for the random dynamics on Γ_D constructed below. To make this distinction clear we shall refer to the former as to the *representation time* (r-time for short) and shall reserve for it the notation t, while the latter will be called the *simulation time* (s-time for short) and will be consequently denoted by s in the sequel.

Consider the following pure jump birth and death type Markovian dynamics on Γ_D, with $\gamma_s = \gamma_s^D$ standing for the current configuration

(*DL:Birth*) With intensity $\langle\langle \mathscr{M} \rangle\rangle(dx)ds$ for $x \in D$ and with intensity $\langle \mathscr{M} \rangle(dl)ds$ for $l \in [\![D]\!]$ set $\gamma_{s+ds} := \gamma_s \oplus x$ and $\gamma_{s+ds} := \gamma_s \oplus l$ respectively.
(*DL:Death*) For each vertex birth site x in γ_s with intensity ds set $\gamma_{s+ds} := \gamma_s \ominus x$. For each line birth site $\mathbb{A}(l[e]) \in e$, $e \in \mathrm{Edges}(\gamma)$ with intensity ds set $\gamma_{s+ds} := \gamma_s \ominus l[e]$.

If none of the above updates occurs we keep $\gamma_{s+ds} = \gamma_s$. It is convenient to perceive the above dynamics in terms of generating random disagreement loops λ and setting $\gamma_{s+ds} := \gamma_s \triangle \lambda$, with the loops of the type $\Delta^{\oplus}[\cdot, \cdot]$ corresponding to the rule (*DL:Birth*) and $\Delta^{\ominus}[\cdot, \cdot]$ to the rule (*DL:Death*).

As a direct consequence of the dynamic representation of the field $\mathscr{A}_D^{\mathscr{M}}$ as developed in Sect. 15.3, we obtain

Theorem 15.2 *The distribution of the polygonal field $\mathscr{A}_D^{\mathscr{M}}$ is the unique invariant law of the dynamics given by* (DL:Birth) *and* (DL:Death). *The resulting s-time stationary process is reversible. Moreover, for any initial distribution of γ_0 the laws of the polygonal fields γ_s converge in variational distance to the law of $\mathscr{A}_D^{\mathscr{M}}$ as $s \to \infty$.*

The uniqueness and convergence statements in the above theorem require a short justification. They both follow by the observation that, in finite volume, regardless of the initial state, the process γ_s spends a non-null fraction of time in the empty state (no polygonal contours). Indeed, this observation allows us to conclude the required uniqueness and convergence by a standard coupling argument, e.g. along the lines of the proof of Theorem 1.2 in [289].

15.5 Adaptive Optimization Scheme for Image Processing

To provide a formal description of our image segmentation procedure we represent the image processed by a continuously differentiable function $\phi : D \to [-1, 1]$ defined on an open bounded convex image domain D. By segmentations of ϕ we shall understand admissible polygonal configurations $\gamma \in \Gamma_D$. Interpreting the contours of γ as curves separating regions of different signs in D we associate with γ two natural sign-functions $s_\gamma^+ : D \to \{-1, +1\}$ and $s_\gamma^- = -s_\gamma^+$. The quality of a segmentation is quantified in terms of an *energy function* $\mathscr{H}[\gamma] := \mathscr{H}[\gamma|\phi]$ which in our case is a positive linear combination of a L_1-type distance (multiple of pixel misclassification ratio), the length element and the number of edges, that is to say

$$\mathscr{H}[\gamma] := \alpha_2 \min\left(\int_D |\phi(x) - s_\gamma^+(x)|dx, \int_D |\phi(s) - s_\gamma^-(x)|dx \right) + \alpha_1 \,\mathrm{length}(\gamma) + \alpha_0 \,\mathrm{card}(\mathrm{Edges}(\gamma)), \quad \alpha_i > 0,\ i = 0, 1, 2, \quad (15.7)$$

although clearly many other natural options are also possible, such as L_p-type metrics or various weighed versions thereof. Our optimization scheme (*OPT*) presented below is based on the (*DL*) evolution as described in Sect. 15.4 above, combined with the following ideas.

- The initial local activity function encodes the gradient information for ϕ.
- In the course of the dynamics, the local activity function undergoes adaptive updates in the spirit of the celebrated Chen algorithm, see [73] and 10.2.4.c in [333].
- The segmentation update proposals are accepted or rejected depending on the energy changes they induce, conforming to the simulated annealing scheme, see [1] for a general reference.

At each time moment $s \geq 0$ in the course of the (OPT) dynamics the local activity function $\mathscr{M}(\cdot\,;\cdot)$ is given by

$$\mathscr{M}_s(l;x) := |\mathbf{e}[l] \times \mathbf{G}_s(x)|, \tag{15.8}$$

where $\mathbf{e}[l]$ is a unit vector along l and $\times$ stands for the usual vector cross product. The vector field $\mathbf{G}_s$ evolves in (OPT) time together with the polygonal configuration γ_s as specified below, with the initial condition

$$\mathbf{G}_0(x) := \nabla\phi(x), \tag{15.9}$$

for practical reasons possibly modified by convolving ϕ with a small variance Gaussian kernel at the pre-processing stage. When combined, the relations (15.8) and (15.9) mean that we promote edges in directions perpendicular to local gradients and proportionally to the gradient lengths. In precise terms, our algorithm admits a description in terms of the following (non-homogeneous) pure-jump Markovian dynamics (OPT) unfolding in time $s \geq 0$.

(OPT:*Initialise*) At time 0 set the initial activity function $\mathscr{M}_0(\cdot\,;\cdot)$ as specified by (15.8) and (15.9) and generate γ_0 according to $\mathscr{A}_D^{\mathscr{M}_0}$.

(OPT:*Birth*) For $\mathscr{M}_s$ given as in (15.8), with intensity $\langle\langle\mathscr{M}_s\rangle\rangle(dx)ds$ for $x \in D$ and with intensity $\langle\mathscr{M}_s\rangle(dl)$ for $l \in [\![D]\!]$ do

[*GenerateDisagreementLoop*] Set $\delta := \gamma_s \oplus x$ and $\delta := \gamma_s \oplus l$ respectively, with λ standing for the respective disagreement loop $\Delta^{\oplus}[x;\gamma]$ or $\Delta^{\oplus}[l;\gamma]$ and with λ^+ and λ^- denoting its respective creation and annihilation phase sub-paths. Note that the disagreement loop is generated according to the current activity measure $\mathscr{M}_s$. Let $\Delta := \mathscr{H}(\delta) - \mathscr{H}(\gamma_s)$ be the energy difference between the current configuration γ_s and its update proposal δ.

[*ActivityUpdate*] Put

$$\begin{aligned}\mathbf{G}_{s+ds}(x) := \mathbf{G}_s(x)\\ + \frac{\exp(-K_s\Delta)-1}{2\pi\sigma_s^2}\int_{\lambda^+}\mathbf{n}[y]\langle\mathbf{n}[y],\mathbf{G}_s(x)\rangle\exp\left(-\frac{\mathrm{dist}^2(x,y)}{2\sigma_s^2}\right)dy\\ + \frac{\exp(K_s\Delta)-1}{2\pi\sigma_s^2}\int_{\lambda^-}\mathbf{n}[y]\langle\mathbf{n}[y],\mathbf{G}_s(x)\rangle\exp\left(-\frac{\mathrm{dist}^2(x,y)}{2\sigma_s^2}\right)dy,\end{aligned}$$

where $\mathbf{n}[y]$ stands for the unit normal to λ at $y \in \lambda$, defined almost everywhere; whereas K_s and σ_s are positive deterministic parameter functions discussed in more detail below.

[*ConfigurationUpdate*] If $\Delta < 0$ then set $\gamma_{s+ds} := \delta$. Otherwise set $\gamma_{s+ds} := \delta$ with probability $\exp(-\beta_s \Delta)$ (*accept update*) and keep $\gamma_{s+ds} = \gamma_s$ with the complementary probability (*reject update*). The parameter function β_s, referred to as the inverse temperature according to the usual terminology, increases in time following the cooling protocol of our simulated annealing.

(*OPT:Death*) With $\mathscr{M}_s$ as given by (15.8), for each vertex birth site x in γ_s with activity ds, and for each line birth site $\mathbb{A}(l[e]) \in e,\ e \in \mathrm{Edges}(\gamma)$ with intensity ds, do

[*GenerateDisagreementLoop*] Set $\delta := \gamma_s \ominus x$ and $\delta := \gamma_s \ominus l[e]$ respectively, with λ standing for the respective disagreement loop $\Delta^{\ominus}[x;\gamma]$ or $\Delta^{\ominus}[l[e];\gamma]$ and with λ^+ and λ^- denoting its respective creation and annihilation phase sub-paths. Note that the disagreement loop is generated according to the current activity measure $\mathscr{M}_s$. Let $\Delta := \mathscr{H}(\delta) - \mathscr{H}(\gamma_s)$ be the energy difference between the current configuration γ_s and its update proposal δ.

[*ActivityUpdate*] Put

$$\begin{aligned}\mathbf{G}_{s+ds}(x) := \mathbf{G}_s(x) &+ \frac{\exp(-K_s\Delta)-1}{2\pi\sigma_s^2}\int_{\lambda^-}\mathbf{n}[y]\langle\mathbf{n}[y],\mathbf{G}_s(x)\rangle\exp\left(-\frac{\mathrm{dist}^2(x,y)}{2\sigma_s^2}\right)dy\\ &+ \frac{\exp(K_s\Delta)-1}{2\pi\sigma_s^2}\int_{\lambda^+}\mathbf{n}[y]\langle\mathbf{n}[y],\mathbf{G}_s(x)\rangle\exp\left(-\frac{\mathrm{dist}^2(x,y)}{2\sigma_s^2}\right)dy.\end{aligned}$$

[*ConfigurationUpdate*] If $\Delta < 0$ then set $\gamma_{s+ds} := \delta$. Otherwise set $\gamma_{s+ds} := \delta$ with probability $\exp(-\beta_s \Delta)$ (*accept update*) and keep $\gamma_{s+ds} = \gamma_s$ with the complementary probability (*reject update*).

Roughly speaking, our optimization dynamics (*OPT*) generates successive updates according to the disagreement loop dynamics (*DL*) driven by the current local activity function $\mathscr{M}_s$, whereupon it updates the activity function in the spirit of the Chen algorithm in [*ActivityUpdate*] phase, and then accepts or rejects the configuration update proposal for γ_s in [*ConfigurationUpdate*] conforming to the simulated annealing paradigm. Note that the activity update is carried out regardless of whether the configuration update proposal has been accepted or not. This is natural because in the activity update step the original and new configuration are compared for quality and then, along the disagreement segments present in the better of the two configurations, the normal component of the local gradient field is reinforced and, likewise, the normal component is subject to fading along the disagreement segments present in the worse configuration. The strength of this reinforcement/fading depends exponentially on the energy difference between the original configuration and its update, with rate controlled by time-dependent parameter K_s, which should increase over time starting from a low level to avoid erratic reinforcements induced by the initially chaotic nature of the early stage polygonal configurations γ_s. To keep the local activity function smooth we smear the activity updates over the domain by convolving them with a Gaussian kernel of time-dependent standard deviation parameter σ_s, as made precise in the [*ActivityUpdate*] formulae above. The

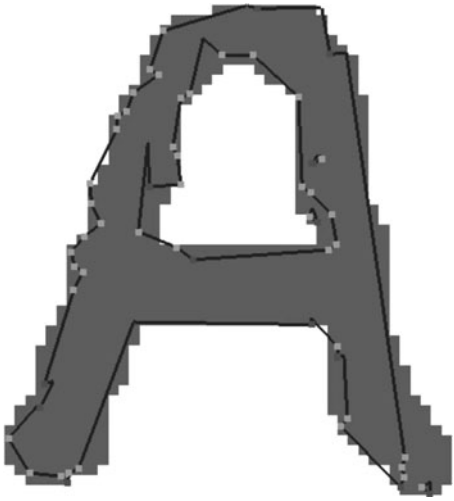

Fig. 15.2 Segmented handwritten A (30000 updates)

parameter σ_s should decrease over time to pass from global shape approximation to fine detail tuning at the later stages of the (OPT) dynamics. The update proposals for the polygonal configurations are accepted or rejected according to the standard simulated annealing scheme with time-dependent inverse temperature parameter β_s which increases over time—to be precise, our software employs a linear cooling schedule $\beta_s = \beta s$ for some constant $\beta > 0$.

15.6 Results and Discussion

In this final section we present applications of our algorithm on sample images. The software, implemented in D programming language, is in a rather early stage of development and will be further optimised. The segmentations shown in Figs. 15.2, 15.3 and 15.4 have been obtained after about 30000 (accepted) updates under a linear cooling schedule, with mean execution time 0.05 sec per single update on Intel Pentium M 2 GHz CPU and 2 GB RAM memory.

A large number of segmentation techniques are available in the literature. But, there does not exist a general algorithm that can perform the segmentation task for all images. Classification of image segmentation methods can be divided into several categories. Starting with the simplest one, the thresholding method, that uses a global property of the image, usually intensity, to classify individual pixels from the image as object pixels, if the value of the pixels property exceeds threshold value, or as background pixels otherwise. The main disadvantage of the method is a narrow range of application, because it works only for a subclass of images in which objects are distinct from background in intensity. The adjustment of the threshold parameter is also a nontrivial task and often requires human interaction. Another well known method is the K-means algorithm [293]. It is an unsupervised clustering algorithm that classifies the pixels from the image into multiple classes based on their inherent

Fig. 15.3 Segmented handwritten B (30000 updates)

Fig. 15.4 Segmented gingerbread-man (30000 updates)

distance from each other. For small values of k the algorithm gives good results, but for larger values of k, the segmentation is very coarse, many clusters appear in the images at discrete places. Selection of parameter k is crucial in that algorithm and inappropriate choice may yield wrong results.

One of the most popular methods in segmentation uses morphological approach: the watershed transformation. That approach was introduced in [34] and consists of placing a spring of water in each selected region, the water will relief from sources, and construct barriers when water from different sources meet. The resulting barriers are the segmentation of the image. The main disadvantage of the algorithm is

the need of human interaction to locate points where flooding should start. Another group of algorithms: the Markov random fields (MRF)-based methods are of great importance, for their ability to model a prior belief about the continuity of image features such as textures, edges or region labels [457], but obtain unsatisfied results when the prior knowledge is taken seriously.

The approach described here uses models that operate on the pixel level. Alternative intermediate level methods focus on the partition of the image that is the outcome of a segmentation. Green [190] and Møller and Skare [313] propose Voronoi-based models, and [318] suggests triangulations. One of the main advantage of our method is a higher conceptual level than most of listed algorithms i.e. the real world is not a collection of pixels and as we do not know what is in the image we cannot model the objects. The algorithm achieves reasonable global behaviour. Another benefit from our algorithm is easy and fast implementation. The drawbacks of our method can be seen around the edges, which will require more finetuning in the future.

Acknowledgements We gratefully acknowledge the support from the Polish Minister of Science and Higher Education grant N N201 385234 (2008–2010).

References

10. ARAK, T.: On Markovian random fields with finite number of values, *4th USSR-Japan symposium on probability theory and mathematical statistics, Abstracts of Communications*, Tbilisi (1982).
11. ARAK, T., SURGAILIS, D.: Markov Fields with Polygonal Realizations, *Probab. Th. Rel. Fields* **80**, 543-579 (1989).
12. ARAK, T., SURGAILIS, D.: Consistent polygonal fields, *Probab. Th. Rel. Fields* **89**, 319-346 (1991).
13. ARAK, T., CLIFFORD, P., SURGAILIS, D.: Point-based polygonal models for random graphs, *Adv. Appl. Probab.* **25**, 348-372 (1993).
34. BEUCHER, S., LANTUJOUL, C.: Use of watersheds in contour detection. *In International workshop on image processing, real-time edge and motion detection* (1979).
73. CHEN, K.: Simple learning algorithm for the traveling salesman problem, *Phys. Rev. E* **55**, 7809-7812 (1997).
79. CLIFFORD, P., AND MIDDLETON, R.D.: Reconstruction of polygonal images. *J. Appl. Stat.* **16**, 409–422 (1989).
190. GREEN, P.: Reversible jump MCMC computation and Bayesian model determination. *Biometrika* 82(4), 711732 (1995).
256. KLUSZCZYŃSKI, R., LIESHOUT, M.N.M. VAN, SCHREIBER, T.: An algorithm for binary image segmentation using polygonal Markov fields. In: F. Roli and S. Vitulano (Eds.), Image Analysis and Processing, Proceedings of the 13th International Conference on Image Analysis and Processing. *Lecture Notes in Comput. Sci.* **3615**, 383-390 (2005).
257. KLUSZCZYŃSKI, R., LIESHOUT, M.N.M. VAN, SCHREIBER, T.: Image segmentation by polygonal Markov fields. *Ann. Inst. Statist. Math.*, **59**, 465-486 (2007).
289. LIGGETT, T.: *Interacting particle systems*. Springer-Verlag, New York (1985).
293. LLOYD, S.P.: Least square quantization in PCM. *IEEE Trans. Inf. Theory*, 28(2), 129137 (1982).
313. MOLLER, J., SKARE, O.: Bayesian image analysis with coloured Voronoi tesselations and a view to applications in reservoir modelling. *Stat. Model.* 1, 213232 (2001).
318. NICHOLLS, G.K.: Bayesian image analysis with Markov chain Monte Carlo and coloured continuum triangulation models. *J. R. Stat. Soc., Ser. B, Stat. Methodol.* 60, 643659 (1998).
319. NICHOLLS, G.K.: Spontaneous magnetization in the plane, *Journal of Statistical Physics*, **102**, 1229-1251 (2001).
333. PERETTO, P.: *An Introduction to the modeling of neural networks*, Collection Aléa-Saclay: Monographs and Texts in Statistical Physics 2, Cambridge University Press (1992).
377. SCHREIBER, T.: Random dynamics and thermodynamic limits for polygonal Markov fields in the plane, *Advances in Applied Probability* **37**, 884-907 (2005).
378. SCHREIBER, T.: Dobrushin-Kotecký-Shlosman theorem for polygonal Markov fields in the plane, *Journal of Statistical Physics*, **123**, 631-684 (2006).
379. SCHREIBER, T.: Non-homogeneous polygonal Markov fields in the plane: graphical representations and geometry of higher order correlations, *Journal of Statistical Physics*, **132**, 669-705 (2008).
380. SCHREIBER, T., LIESHOUT, M.N.M. VAN: Disagreement loop and path creation/annihilation algorithms for binary planar Markov fields with applications to image segmentation, *submitted* (2008).
395. SURGAILIS, D.: Thermodynamic limit of polygonal models, *Acta applicandae mathematicae*, **22**, 77-102 (1991).
424. LIESHOUT, M.N.M. VAN, SCHREIBER, T.: Perfect simulation for length-interacting polygonal Markov fields in the plane, *Scand. Journal of Statistics*, **34**, 615-625 (2007).
448. WINKLER, G.: Image analysis, random fields and Markov chain Monte Carlo methods, A mathematical introduction, *2nd ed. Applications of Mathematics, Stochastic Modelling and Applied Probability* **27**. Springer-Verlag, Berlin (2003).
457. YANG, F., JIANG, T.: Pixon based image segmentation withMarkov random fields. *IEEE Trans. Image Process.* 12(12), 15521559 (2003).